RbB_3Si_3: An Alkali Metal Borosilicide that is Metastable and Superconducting at 1 atm

Xiangyue Cui,[1] Katerina P. Hilleke,[2] Xiaoyu Wang,[2] Mingchun Lu,[3] Miao Zhang,[1, 2, *] Eva Zurek,[2,*] Wenjing Li,[1] Dandan Zhang,[1] Yan Yan,[2, 4] Tiange Bi[2]

[1]*Department of Physics, School of Sciences, Beihua University, Jilin 132013, China*
[2]*Department of Chemistry, State University of New York at Buffalo, Buffalo, NY 14260-3000, United States*
[3]*Department of Aeronautical Engineering Professional Technology, Jilin Institute of Chemical Technology, Jilin 132102, China*
[4]*School of Sciences, Changchun University, Changchun 130022, China*

*Corresponding author.
E-mail: zhangmiaolmc@126.com (Miao Zhang); ezurek@buffalo.edu (Eva Zurek).

Abstract

The stability, electronic structure and potential superconductivity in AB_3Si_3 (A = Na, K, Rb, and Cs) compounds that assume the clathrate-based sodalite structure whose frameworks consists of covalent B-Si bonds is investigated via first-principles calculations. This structure type has recently been predicted in a number of high temperature superconducting hydrides, but these are only stable under megabar pressures. Herein, we predict a novel superconducting phase, RbB_3Si_3, that could be synthesized under pressures that are a factor of ten smaller, ~10 GPa, and quenched to atmospheric conditions. Electron-phonon coupling calculations predict that RbB_3Si_3 possesses a superconducting critical temperature, T_c, of 14 K at 1 atm. The dynamic stability of RbB_3Si_3 and CsB_3Si_3 at ambient pressure can be explained by considering the chemical pressure exerted on the B-Si framework that is caused by the size effect of the alkali metal atom.

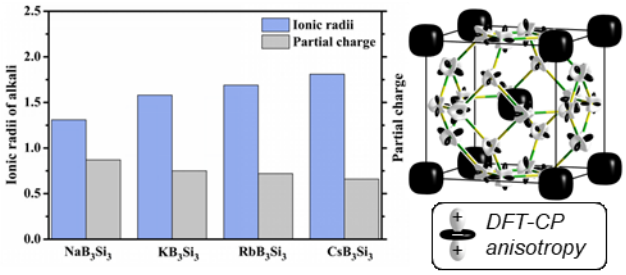

TOC Graphic

Introduction

The last few years have witnessed tremendous advances in the discovery of novel phonon-mediated superconductors, with measured record high superconducting critical temperatures (T_cs) first in SH_3 (T_c of 203 K at 150 GPa)[1,2], and less than five years later in LaH_{10} (T_c up to 260 K near 200 GPa)[3]. The search for superconductivity in compressed hydrides was inspired by Ashcroft's conjecture[4] that such systems would be good candidates for conventional high-T_c materials, and many binary systems have been studied theoretically.[5-12] Remarkably, the most recent experimental discoveries[13,14] were driven by theoretical predictions of near room temperature superconductivity in an *Fm-3m* symmetry LaH_{10} phase wherein the hydrogen lattice assumes a three-dimensional clathrate structure and the metal atoms reside in the center of the cages.[15,16] This clathrate is comprised of H_{32} polyhedra composed of six square and twelve hexagonal faces wherein the weak H-H bonds give rise to the remarkably high electron-phonon coupling. An analogous sodalite-like H_{24} cage composed of six square and eight hexagonal faces[17] has been proposed to be stable or metastable for MgH_6 (300 GPa),[18] CaH_6 (150 GPa),[19] ScH_6 (350 GPa),[20] YH_6 (120 GPa),[21] and LaH_6 (100 GPa)[16] at the pressures given in the braces. These alkaline and rare earth hexahydrides have also been predicted to have high T_c values.[17] Unfortunately, when the pressure is released, none of them are stable, and will decompose into the classic-stoichiometry hydrides known to exist at 1 atm, as well as molecular H_2.

On the other hand, several metal silicide clathrates, largely based on Ba_8Si_{46} (T_c = 8 K),[22] including $(Na,Ba)_xSi_{46}$ (T_c = 4 K),[23] and $Ba_8Al_6Si_{40}$ (T_c = 4.7 K)[24] that are superconducting and stable at 1 atm have been synthesized. Since these assume the clathrate I structure type, we wondered if metal silicides that adopt a sodalite-like structure, of which none are currently known, could be stabilized under pressure and quenched to atmospheric conditions, resulting in superconducting candidate structures analogous to the metal hexa-hydrides?

Additionally, the small cages in the borosilicide $K_7B_7Si_{39}$,[25] another example of

the clathrate I crystal structure, hint that the addition of boron to metal silicides could allow for the inclusion of smaller metals in the clathrate cages. This suggestion is mirrored by theoretical studies that have proposed that small ions may be inserted into carbon clathrate cages wherein some of the carbon atoms have been substituted with boron.[26] This work inspired the computational prediction of an SrB_3C_3 compound in the bipartite sodalite structure, which was computed to be thermodynamically stable from 50 to at least 200 GPa.[27] The calculations further suggested that at 1 atm SrB_3C_3 could be a superconductor, and its Vickers hardness, H_v, was estimated as 24 GPa. Remarkably, this phase was subsequently synthesized under pressure, and quenched to 1 atm in an inert atmosphere.[27] Other non-hydride sodalite-like phases that have recently been theoretically predicted include: BN frameworks, $X(BN)_6$, X = Al, Si, Cl, with T_c and H_v as high as 47 K and 35 GPa;[28] $LiBC_{11}$ and $Li_2B_2C_{10}$ semiconductors with H_v of 49 GPa and 38 GPa;[29] and doped carbides such as NaC_6, AlC_6 and LiC_6 with T_cs reaching as high as 100 K.[30] These investigations inspired us to theoretically study the stability and properties of sodalite-like compounds with the formula AB_3Si_3 (A= Na, K, Rb and Cs), as shown in Figure 1(a).

Methods

The AB_3Si_3 structures considered herein are isotypic with the previously predicted SrB_3C_3 cubic bipartite sodalite phase. They resemble the aforementioned MH_6 superhydrides, except the silicon or carbon atoms are bonded only to boron atoms (and vice versa), with the metal atoms found in the center of the cage. This lowers the symmetry from *Im-3m* in the superhydrides to *Pm-3n* (space group No. 223, with two formula units per cell) in the group 14-based clathrates. Density functional theory calculations, whose details are given in the Supporting Information (SI), were employed to relax the structures within the pressure range of 0 - 200 GPa. At atmospheric pressures, the optimized lattice parameters of NaB_3Si_3, KB_3Si_3, RbB_3Si_3, and CsB_3Si_3 were 5.805, 5.863, 5.911, and 5.983 Å, with alkali metals occupying the 2*a* (0, 0, 0), boron atoms occupying the 6*d* (0, 0.5, 0.25), and Si atoms occupying the 6*c* (0.5, 0, 0.25) Wyckoff sites, respectively.

Results & Discussion

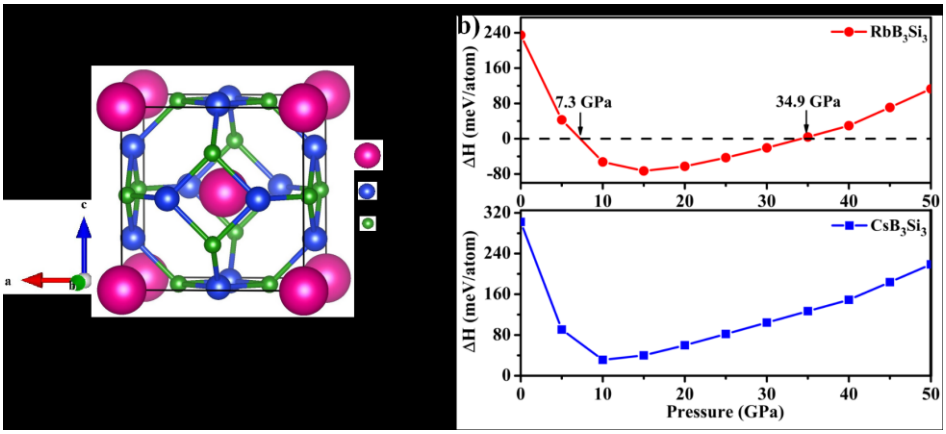

Figure 1. (a) Crystal structures of AB_3Si_3, where A refers to an alkali metal (Na, K, Rb and Cs). Pink, blue, and green spheres represent the alkali metals, Si and B atoms, respectively. (b) Calculated enthalpy of formation, ΔH, of RbB_3Si_3 and CsB_3Si_3 as a function of pressure. For Rb we used the enthalpies of the *bcc* → *fcc* →$I4_1/amd$ → *Cmca* → *dhcp* structures, with the phase transitions occurring at 8.2, 15.1, 41.0 and 146.8 GPa, respectively. For Cs we used the enthalpies of the *fcc* → $I4_1/amd$ → *Cmca* → *dhcp* structures, with the phase transitions occurring at 3.6, 10.7 and 49.5 GPa, respectively. The phases of the other elements employed to calculate ΔH are given in the SI.

The phase stabilities of AB_3Si_3 (A = Na, K, Rb and Cs) compounds were systematically investigated by calculating the enthalpy of formation, ΔH, from the elemental phases. As shown in Figure 1(b), ΔH for RbB_3Si_3 was negative within the pressure range of 7 - 35 GPa, and ΔH was found to be +31 meV/atom for CsB_3Si_3 at 10 GPa. As shown in Figure S5, the ΔH of NaB_3Si_3 is positive within the pressure range considered, whereas the ΔH for KB_3Si_3 is negative between 7 - 37 GPa. Phonon calculations were carried out to study the dynamic stability of these phases. The phases with larger alkali earth metals, RbB_3Si_3 and CsB_3Si_3, were found to be local minima that did not show any imaginary frequency modes throughout the Brillouin Zone at ambient pressure, and at 10 GPa (Figure S6). NaB_3Si_3 and KB_3Si_3, on the other hand, were not dynamically stable at either one of these pressures, with the number of imaginary modes and their magnitude increasing under pressure. It should be pointed out that there are documented examples where high pressure

synthesis techniques have been successful in making materials whose ΔH was computed to be positive under pressure at 0 K in the static lattice approximation, for example Ca_2H_5[31] (ΔH = +20 meV/atom above the 20 GPa convex hull), and hydrides of phosphorus[32] (ΔH > 30 meV/atom above the convex hull).[33,34] These results suggest that both RbB_3Si_3 and CsB_3Si_3 could potentially be synthesized at moderate pressures and quenched to atmospheric conditions, akin to the recent findings for SrB_3C_3.

In order to get a better understanding of the driving forces behind the phase stability, a DFT-Chemical Pressure (CP) analysis,[35] which reveals the internal tensions present in a crystalline compound, was performed on the 1 atm structures. In the CP scheme, atom-centered spherical harmonic functions are plotted so that negative CP, reflective of a local desire for contraction of the structure, is indicated by black lobes, with white lobes corresponding to positive CP and a local desire for expansion of that contact. In the CP schemes of all four AB_3Si_3 compounds the most striking feature is the large negative CP displayed surrounding the alkali metal atom, an indication that it is too small for its coordination environment within the B-Si cage, as shown in Figure 2. Consequently, shrinking the B-Si cage would be a stabilizing effect for the alkali metal atom, but the positive B-Si CPs directed along the B-Si cage edges serve to balance this desire. These positive CPs indicate that the B-Si contacts within the cage are too short already, so that shrinking the cage to accommodate the size of the alkali metal atom would only exacerbate this tension. The B-Si bond lengths increase slightly as the size of the alkali ion increase, measuring 2.05 Å for NaB_3Si_3 to 2.12 Å for CsB_3Si_3.

While the general features of the CP scheme are shared across all four compounds, the magnitude of the negative CP on the alkali metal atoms changes with the size of the A atom. Na, the smallest of the four alkalis, has the poorest fit inside the B-Si cage, reflected in the extremely large negative CP surrounding the Na atoms. As the size of the A atom increases, from Na to K, to Rb, and finally to Cs, the magnitude of the negative CP lessens drastically, indicating an improved size match between the space within the B-Si cage and the alkali metal atom that fills it. These observations are in

line with the calculated phonon band structures (Figure S6): RbB_3Si_3 and CsB_3Si_3 are dynamically stable at ambient pressure, as befits the larger alkali metals being better able to fill the B-Si cage voids, whereas KB_3Si_3 displays one imaginary mode with a small magnitude near the M-point and NaB_3Si_3 exhibits many imaginary modes with a large amplitude.

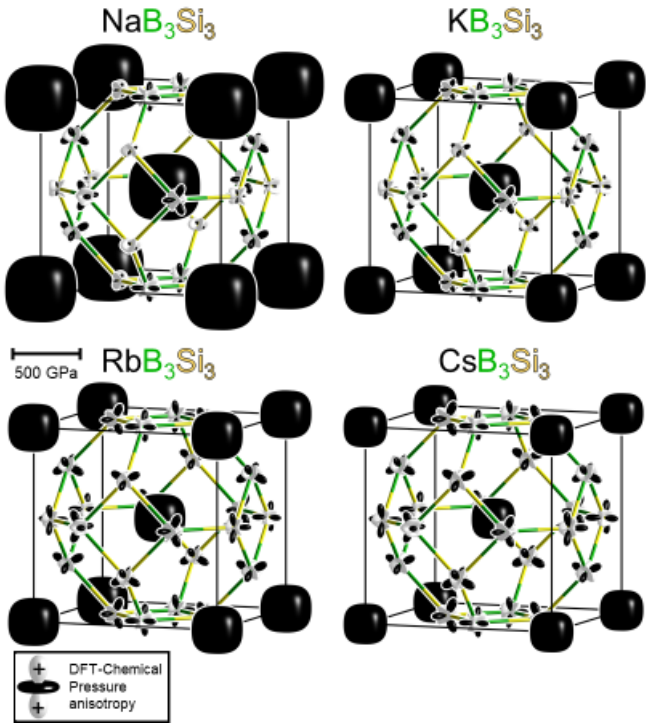

Figure 2. Chemical Pressure (CP) schemes of AB_3Si_3 (A=Na, K, Rb, Cs) at 0 GPa. Negative pressures (black) surround the A atoms, indicating the too-large coordination environment of the B-Si cage, with positive pressures (white) between the B and Si atoms. Increasing the size of the alkali metal atom reduces the magnitude of the negative CP, as the larger atoms obtain a better fit within the B-Si cages.

A $[Si_3B_3]^{3-}$ cubic bipartite sodalite phase would possess a closed electronic shell and therefore be an insulator at low pressures. Therefore, doping the neutral cage by one electron per formula unit - the formal charge transferred from the alkali metal - would render it a hole conductor. The calculated Bader charges (Table S2) suggest that the charge transfer decreases slightly as the size of the alkali increases. The electronic band structure and density of states of RbB_3Si_3 at 1 atm, illustrated in Figure 3, verifies the expectation of metallicity. Doping with two more electrons

would move the Fermi level (E_F) up in energy into the gap. The structural and electronic similarities between RbB_3Si_3 and SrB_3C_3[27] are evident when comparing their band structures, e.g. the way the bands "run" and disperse, as well as their projections onto atom-centered orbitals. The bands crossing E_F are primarily of boron and silicon *p*-character, and the density of states at E_F is high. The presence of a flat band near E_F at the M-point, and steep bands crossing E_F elsewhere in the Brillouin Zone are suggestive of superconductivity, as first proposed by Zhu *et al.*[27] The Fermi surface, illustrated in Figure S7, is comprised of a number of straight parallel pieces that appear to be well nested.

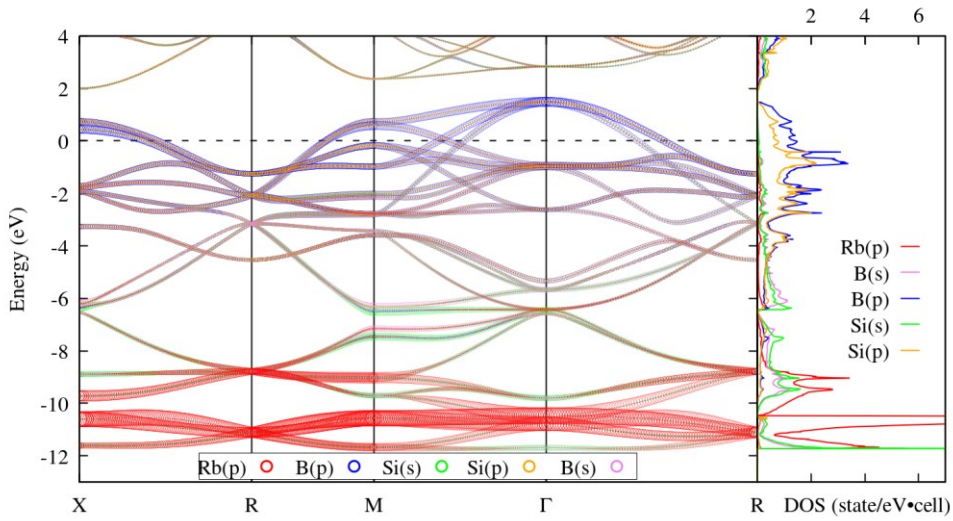

Figure 3. Electronic band structure for RbB_3Si_3 at 0 GPa projected onto atomic orbitals that are represented by different colored circles whose radius is proportional to their contribution. The projected density of states (DOS) is shown in the right panel.

In order to verify the potential superconductivity of RbB_3Si_3, we calculated the electron-phonon coupling constant, $\lambda = 0.74$, logarithmic average of the phonon frequencies, $\omega_{log} = 333$ K, and estimated T_c via the Allen-Dynes modified McMillan equation[36] using a Coulomb pseudopotential, μ^*, value of 0.1. These calculations suggest that RbB_3Si_3 would be a conventional superconductor with a T_c of 14.0 K at ambient pressures. The anisotropic superconducting gap of RbB_3Si_3 obtained with the Eliashberg formalism is provided in Figure S10. The projected phonon densities of

states, illustrated in Figure 4, shows that the vibrations associated with the motion of the heavy Rb atoms have a low frequency, as expected. Visualization of the phonons reveals that the relatively flat band around 120 cm^{-1} is due to the rattling mode of the Rb atom within the clathrate-like cages. This mode, however, does not contribute towards λ, in accordance with the fact that Rb-character is not present in the electronic states near E_F (Figure 3). The electron-phonon coupling arises from the vibrations of the B and Si atoms, with the modes below 375 cm^{-1} that result in nearly 2/3 of λ being primarily due to the heavier Si atoms, and the modes between 375-750 cm^{-1} that are primarily due to the lighter B atoms giving rise to the remaining 1/3. The phonon bands with the largest linewidths are a hextuply degenerate band with a frequency of ~101 cm^{-1} at the R-point, and a set of bands that, at the M-point, yields two doublets with frequencies of ~101 cm^{-1} and ~103 cm^{-1}. These modes arise from asymmetric in-plane stretches of the B_2Si_2 square faces that, at the R-point, are also coupled with out-of-plane tilting motions in alternating layers of B_2Si_2 square faces. At the M-point, these modes also result in a "breathing motion" of the B_3Si_3 hexagonal faces. Calculations on the first sodalite-like high-temperature superconducting hydride to be predicted, CaH_6, revealed that the largest phonon linewidth arose from the in-plane breathing and rocking vibrations of the hydrogen atoms within the square faces.[19] The breathing of H_4 square units in CaH_6 is analogous to the B_2Si_2 square stretches in RbB_3Si_3, however, the B_2Si_2 squares exhibit out-of-plane tilting motions instead of the in-plane rocking mode of the H_4 squares. The T_c of CsB_3Si_3 is likely to be slightly lower than that of RbB_3Si_3 because the lower frequency vibrations of the heavier alkali metal atom will result in a smaller ω_{log}.

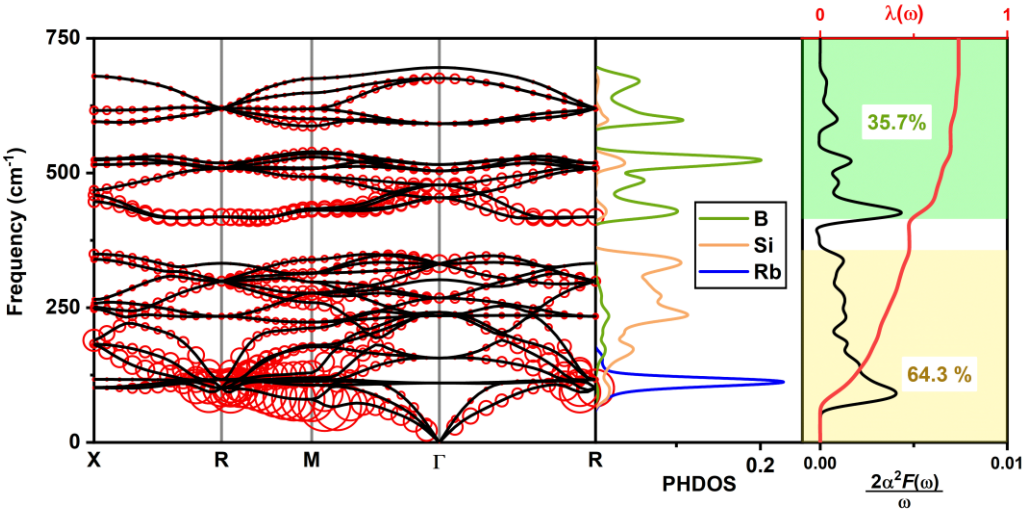

Figure 4. Phonon band structure, projected phonon density of states, Eliashberg spectral function, and the electron phonon integral, λ(ω), for RbB_3Si_3 at ambient pressure. Red circles indicate the electron phonon coupling constant, λ_{qv}, at mode *v* and wave-vector *q* (phonon linewidths), and their radius is proportional to the strength.

Conclusions

In summary, our detailed first-principles calculations have shown that the size of the A atom in the metal borosilicides, AB_3Si_3, that assume the bipartite sodalite structure is a key factor for determining if they can be metastable at 1 atm. A chemical pressure analysis showed that in the case of the alkali metals Cs had the best, and Na the worst fit within the B-Si cage, with the negative chemical pressure displayed by the alkali metals indicating the site's preferential occupation by a larger atom. Accordingly, both RbB_3Si_3 and CsB_3Si_3 were dynamically stable at 0 - 10 GPa, whereas NaB_3Si_3 and KB_3Si_3 were not. Because Fr is the only metal with a larger ionic radius than Cs, it might fit even better within the B-Si cage, however its extreme radioactivity and scarcity precludes it from any practical use. At 10 GPa the enthalpy of formation of RbB_3Si_3 with respect to the elemental phases is negative, whereas CsB_3Si_3 is only slightly disfavored, suggesting that these compounds could potentially be synthesized at mild pressures and quenched to 1 atm. Electron-phonon calculations predict that RbB_3Si_3 would be a conventional superconductor with a T_c of ~14.0 K at ambient pressures. This is comparable to other well-known phonon mediated

superconductors such as Nb_3Ge (17.0 K)[37], and Nb_3Sn (18.0 K)[38], but lower than the record set by MgB_2 (39 K)[39].

Notes

The authors declare no competing financial interests.

Acknowledgements

This research was supported by the Natural Science Foundation of China (Grant Nos. 11504007 and 11404035), and the Scientific and Technological Research Project of the ‘‘13th Five-Year Plan’’ of Jilin Provincial Education Department (Grant Nos. 2016049, JJKH20200031KJ, and JJKH20180941KJ). E. Z. and X. W. acknowledge the NSF (DMR-1827815) for financial support. K. H. is thankful to the U.S. Department of Energy, National Nuclear Security Administration, through the Capital-DOE Alliance Center under Cooperative Agreement No. DE-NA0003858 for financial support. We acknowledge the Center for Computational Research (CCR) at SUNY Buffalo for computational support.[40] The work was also supported by the Foster Program of Youth Research Innovation Team in Beihua University.

Supporting Information

The Supporting Information is available free of charge on the ACS Publications website. It includes the details of the computations, structural parameters, computed Bader charges, B-Si distances and phonon band structures of AB_3Si_3 (A = Na, K, Rb and Cs), the enthalpies of formation of NaB_3Si_3 and KB_3Si_3, as well as the Fermi surface of RbB_3Si_3.

Reference

(1) Drozdov, A. P.; Eremets, M. I.; Troyan, I. A.; Ksenofontov, V.; Shylin, S. I. Conventional superconductivity at 203K at high pressure at high pressures in the sulfur hydride system. *Nature* **2015**, *525*, 73–76.

(2) Yao, Y.; Tse, J. S. Superconducting Hydrogen Sulfide. *Chem. Eur. J.* **2018**, *24*, 1769–1778.

(3) Hemley, R.; Ahart, M.; Liu, H.; Somayazulu M. Road to room-temperature superconductivity: T_c above 260 K in lanthanum superhydride under pressure.
Proceedings of the International Symposium - Superconductivity and Pressure: A Fruitful Relation ship on the Road to Room Temperature Superconductivity, **2018**, May 21-22, pp. 199-213.

(4) Ashcroft. N. W. Hydrogen dominant metallic alloys: High temperature superconductors? *Phys. Rev. Lett.* **2004**, *92*, 187002.

(5) Bi, T.; Zarifi, N.; Terpstra, T.; Zurek, E. The search for superconductivity in high pressure hydrides. *Reference Module in Chemistry, Molecular Sciences and Chemical Engineering.* **2019**, Elsevier, pp. 1-36.

(6) Wang, H.; Li X.; Gao, G.; Li, Y.; Ma, Y. Hydrogen-rich superconductors at high pressure. *WIREs Comput. Mol. Sci.* **2018**, *8*, 1–13.

(7) Zhong, X.; Wang, H.; Zhang, J.; Liu, H.; Zhang, S.; Song, H.; Yang, G.; Zhang, L.; Ma, Y. Tellurium hydrides at high pressures: High-temperature superconductors. *Phys. Rev. Lett.* **2016**, *116*, 057002.

(8) Gao, G.; Oganov, A. R.; Li, P.; Li, Z.; Wang, H.; Cui, T.; Ma, Y.; Bergara, A.; Lyakhov, A. O.; litaka, T.; et al. High-pressure crystal structures and superconductivity of stannane (SnH_4). *Proc. Natl. Acad. Sci. U. S. A.* **2010**, *107*, 1317–1320.

(9) Zhang, S.; Wang, Y.; Zhang, J.; Liu, H.; Zhong, X.; Song, H.; Yang, G.; Zhang, L.; Ma, Y. Phase diagram and high-temperature superconductivity of compressed selenium hydrides. *Sci. Rep.* **2015**, *5*, 15433.

(10) Fu, Y.; Du, X.; Zhang, L.; Peng, F.; Zhang, M.; Pickard, C. J.; Needs, R. J.; Singh, D. J.; Zheng, W.; Ma, Y. High-pressure phase stability and superconductivity of pnictogen hydrides and chemical trends for compressed hydrides. *Chem. Mater.* **2016**, *28*, 1746–1755.

(11) Semenok, D. V.; Kvashnin, A. G.; Kruglov, I. A.; Oganov, A. R. Actinium hydrides AcH_{10}, AcH_{12}, and AcH_{16} as high-temperature conventional superconductors. *J. Phys. Chem. Lett*. **2018**, *9*, 1920-1926.

(12) Shamp, A.; Zurek, E. Superconducting high-pressure phases composed of hydrogen and iodine. *J. Phys. Chem. Lett*. **2015**, *6*, 4067-4072.

(13) Somayazulu, M.; Ahart, M.; Mishra, A. K.; Geballe, Z. M.; Baldini, M.; Meng, Y.; Struzhkin, V. V.; Hemley, R. J. Evidence for superconductivity above 260 K in lanthanum superhydride at megabar pressures. *Phys. Rev. Lett.* **2019***, 122*, 027001.

(14) Drozdov, A. P.; Kong, P. P.; Minkov, V. S.; Besedin, S. P.; Kuzovnikov, M. A.; Mozaffari, S.; Balicas, L.; Balakirev, F. F.; Graf, D. E.; Prakapenka, V. B.; et al. Superconductivity at 250 K in lanthanum hydride under high pressures. *Nature* **2019**, *569*, 528-531.

(15) Liu, H.; Naumov, I. I; Hoffmann, R.; Ashcroft, N. W.; Hemley, R. J. Potential high-Tc superconducting lanthanum and yttrium hydrides at high pressure. *Proc. Natl. Acad. Sci. U. S. A.* **2017**, *114*, 6990–6995.

(16) Peng, F.; Sun, Y.; Pickard, C. J.; Needs, R. J.; Wu, Q.; Ma, Y. Hydrogen clathrate structures in rare earth hydrides at high pressures: Possible route to room-temperature superconductivity. *Phys. Rev. Lett.* **2017**, *119*, 107001.

(17) Zurek, E.; Bi, T. High-temperature superconductivity in alkaline and rare earth polyhydrides at high pressure: A theoretical perspective. *J. Chem. Phys.* **2019**, *150*, 050901.

(18) Feng, X.; Zhang, J.; Gao, G.; Liu, H.; Wang, H. Compressed sodalite-like MgH_6 as a potential high-temperature superconductor. *RSC Adv.* **2015**, *5*, 59292–59296.

(19) Wang, H.; Tse, J. S.; Tanaka, K.; litaka, T.; Ma, Y. Superconductive sodalite-like clathrate calcium hydride at high pressures. *Proc. Natl. Acad. Sci. U. S. A.* **2012**, *109*, 6463–6466.

(20) Ye, X.; Zarifi, N.; Zurek, E.; Hoffmann, R.; Ashcroft, N. W. High hydrides of scandium under pressure: Potential superconductor. *J. Phys. Chem. C.* **2018**, *122*, 6298–6309.

(21) Li, Y.; Hao, J.; Liu, H.; Tse, J. S.; Wang, Y.; Ma, Y. Pressure-stabilized superconductive yttrium hydrides. *Sci. Rep.* **2015**, *5*, 9948.

(22) Yamanaka, S.; Enishi, E.; Fukuoka, H.; Yasukawa, M. High-pressure synthesis of a new

silicon clathrate superconductor, Ba_8Si_{46}. *Inorg. Chem.* **2000**, *39,* 56-58.

(23) Kawaji, K.; Horie, H.; Yamanaka, S.; Ishikawa, M. Superconductivity in the silicon clathrate compound $(Na,Ba)_xSi_{46}$. *Phys. Rev. Lett.;* **1995**, *74,* 1427-1429.

(24) Li, Y.; Garcia, J.; Chen, N.; Liu, L.; Li, F.; Wei, Y.; Bi, S.; Cao, G.; Feng, Z.S. Superconductivity in Al-substituted Ba_8Si_{46} clathrates. *J. Appl. Phys.* **2013**, *113*, 203908.

(25) Jung, W.; Lörincz, J.; Ramlau, R.; Borrmann, H.; Prots, Y.; Haarmann, F.; Schnelle, W.; Burkhardt, U.; Baitinger, M, Grin, Y. $K_7B_7Si_{39}$, a borosilicide with the clathrate I structure. *Angew. Chem. Int. Ed.* **2007,** *46,* 6725-6728.

(26) Zeng, T.; Hoffmann, R.; Nesper, R.; Ashcroft, N. W.; Strobel, T. A.; Proserpio, D. M. Li-filled, B-substituted carbon clathrates. *J. Am. Chem. Soc.* **2015**, *137*, 12639-12652.

(27) Zhu, L.; Borstad, G. M.; Liu, H.; Guńka, P. A.; Guerette, M.; Dolyniuk, J. A.; Meng, Y.; Greenberg, E.; Prakapenka,V. B.; Chaloux, B. L.; et al. Carbon-boron clathrates as a new class of sp^3-bonded framework materials. *Sci. Adv*. **2020**, *6*, 8361.

(28) Li, X.; Yong X.; Wu, M.; Lu, S.; Liu, H.; Meng, S.; Tse, J. S. Hard BN clathrate superconductors. *J. Phys. Chem. Lett*. **2019**, *10*, 2554-2560.

(29) Feng, X.; Zhang, X.; Liu, H.; Qu, X.; Redfern, S. A. T.; Tse, J. S.; Li, Q. Low-density superhard materials: Computational study of Li-inserted B-substituted closo-carboranes $LiBC_{11}$ and $Li_2B_2C_{10}$. *RSC Adv.* **2016**, *6*, 52695-52699.

(30) Lu, S.; Liu, H.; Naumov, I. I.; Meng, S.; Li, Y.; Tse, J. S.; Yang, B.; Hemley, R. J. Superconductivity in dense carbon-based materials. *Phys. Rev. B* **2016**, *93*, 104509.

(31) Mishra, A. K.; Muramatsu, T.; Liu, H.; Geballe, Z. M.; Somayazulu, M.; Ahart, M.; Baldini, M.; Meng, Y.; Zurek, E.; Hemley, R. J. New calcium hydrides with mixed atomic and molecular hydrogen. *J. Phys. Chem. C* **2018**, *122*, 19370-19378.

(32) Drozdov, A. P.; Eremets, M. I.; Troyan, I. A. Superconductivity above 100 K in PH_3 at high pressures. *arXiv:1508.06224*, **2015**.

(33) Shamp, A.; Terpstra, T.; Bi, T.; Falls, Z.; Avery, P.; Zurek, E. Decomposition products of phosphine under pressure: PH_2 stable and superconducting? *J. Am. Chem. Soc.* **2016**, *138*, 1884-1892.

(34) Bi, T.; Miller, D.; Shamp, A.; Zurek, E. Superconducting phases of phosphorus hydride under pressure: Stabilization by mobile molecular hydrogen. *Angew. Chem. Int. Ed.* **2017**, *56*,

10192-10195.

(35) Fredrickson, D. C. DFT-chemical pressure analysis: Visualizing the role of atomic size in shaping the structures of inorganic materials. *J. Am. Chem. Soc.* **2012**, *134*, 5991-5999.

(36) Allen, P. B.; Dynes, R.C.; Transition temperature of strong-coupled superconductors reanalyzed. *Phys. Rev. B* **1975**, *12*, 905.

(37) Matthias, B. T.; Geballe, T. H.; Willens, R. H.; Corenzwit, E.; Hull Jr, G. W. Superconductivity of Nb_3Ge. *Phys. Rev.* **1965**, *139*, A1501.

(38) Matthias, B. T.; Geballe, T. H.; Geller, S.; Corenzwit, E. Superconductivity of Nb_3Sn. *Phys. Rev.* **1954,** *95*, 1435.

(39) Nagamatsu, J.; Nakagawa, N.; Muranaka, T.; Zenitani, Y.; Akimitsu, J. Superconductivity at 39 K in magnesium diboride. *Nature* **2001**, *410*, 63-64.

(40) Center for Computational Research, University at Buffalo. Available online: http://hdl.handle.net/10477/79221.